Conformational analysis of new 14-membered ring diketal dilactam macrocycles: molecular mechanics, liquid and solid state NMR studies

Denise Dugat, Ag Valade, Bruno Combourieu, J. Guyot

Conformational analysis of new 14-membered ring diketal dilactam macrocycles: molecular mechanics, liquid and solid state NMR studies

Denise Dugat,* Anne-Gaëlle Valade, Bruno Combourieu and Jacques Guyot

Synthèse et Etude de Systèmes à Intérêt Biologique, UMR CNRS 6504, Université Blaise Pascal de Clermont-Ferrand, 63177 Aubière, France

1. Introduction

In the last four decades, conformational analysis of macrocyclic compounds has attracted increasing interest, partly because of the insight it brings on the physical and chemical properties of these systems.

For some years we have been interested in the synthesis[1] and in cationic recognition properties[2] of new diversely substituted 14-membered ring compounds bearing diketal and dilactam functions (Scheme 1). The conformational preferences of these macrocycles according to the nature of their substituents should help to account for the differences observed in their binding abilities. The complexity of the molecules, due to the presence of two different functions and of various substituents, prompted us first to search the literature for proposed shapes for these structures, beginning with the
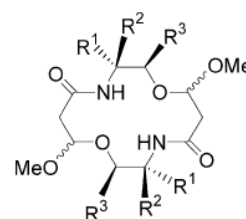
Scheme 1.

unsubstituted 14-membered ring cycloalkane, cyclo-tetradecane.

The conformation of cyclotetradecane was thoroughly investigated using, successively, qualitative analysis,[3] semi-quantitative enthalpy calculations,[4] low temperature NMR,[5] X-ray diffraction,[6] solid state ^{13}C NMR,[7] molecular mechanics methods[8] and vibrational spectroscopy.[9] These studies show that c-$C_{14}H_{28}$ occurs in the solid state as an ordered crystalline phase with a single conformation,[6,7] but in the liquid state the cycloalkane ring loses its conformational homogeneity and occurs in several conformations, among which the crystal conformation is largely
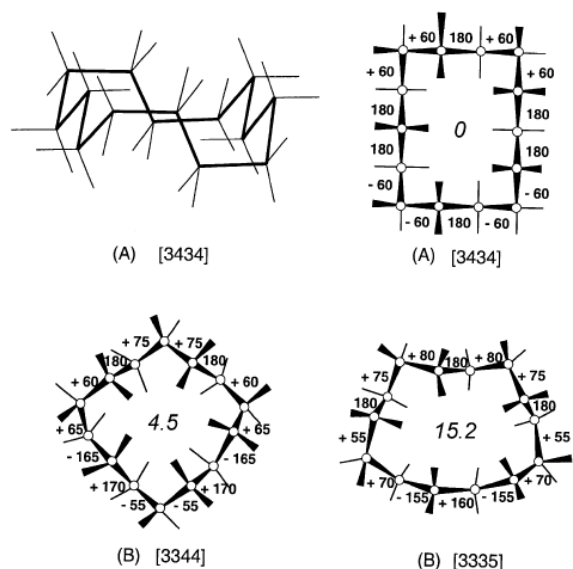
Figure 1. Representations of cyclotetradecane: (A) Side view and top view of the [3434] rectangular conformer;[3a,4] (B) Top views of the [3344] and [3335] quadrangular conformers.[3a] Positive and negative numbers refer to the ring torsion angles[3a] and italic numbers to the relative conformational strain energies (kJ mol^{-1}) given by Snyder[9] after readjustment of the first values calculated by Dale.[4a]

predominant.[4,5,8,9] This first conformer of lowest energy, designated [3434]† or gtggttg′g′tg′g′ttg‡ according to Dale's[4] and Snyder's[9] respective conventions, possesses the ideal strain-free 'rectangular' diamond lattice structure,[3,4,10a] with four 'corners' corresponding to gg or g′g′ sequences and two parallel long chains roughly at van der Waals distance linked at each end by C_2 bridges in a perspective drawing (Fig. 1).[3] Among the conformers detected at higher energy, the second and the eighth ones, named [3344] or gtggtggttg′g′ttg and [3335] or gtggtggtggtttg, respectively, present a 'quadrangular' conformation.[4a,9] The unsymmetrical arrangement gg′ or g′g of two *gauche* bonds of opposite sign, generally excluded in open chains by the 1,5 pentane interaction,[4a] but apparently very common in medium rings,[8] is encountered in several conformers, from the fourth to the seventh, with an increase to ≈100° of one of the two dihedral angles.[8,9]

Simple substituents on cyclotetradecane are assumed not to influence the conformation of the ring itself, except by their bulk.[3a] An alkyl group, particularly a *gem*-dimethyl group, would be preferentially located in a corner position of the

rectangular cyclotetradecane and a symmetrical bi-*gem*-dimethyl substitution would favour the diamond-lattice conformation.[11,12] Replacement of a –CH$_2$– group by –O–, –NR–, –C═O, –C═N–OH, etc. is considered to cause minimal perturbations[3a] and gives the same [3434] conformational preference for: (i) 1-oxa-,[13] 1,3,8,10-tetra-oxa-,[14] 1,8-diaza-,[10b,15] and 1,8-dihydroxy-1,8-diaza-[10b,16] cyclotetradecanes, (ii) cyclotetradecanone,[17,18] cyclotetradecane-1,8-dione,[11,19] cyclotetradecane oxime[20] and tridecanolactone.[21]

Insertion, into the saturated ring chain, of an amide linkage which presents a partial double-bond character, induces some strain in the molecule. The torsion angles adjacent to the amide group are expected to be about 60 and 120° for the extreme case.[22,23] Between the two possible configurations of the NH–CO function, the *trans* one (H *anti* to the carbonyl oxygen atom) is strongly favoured[3b] and is in fact the exclusive conformation for *n*-membered ring lactams in which $n \geq 11$.[24] Studies of 1-azacyclotetradecane-2-one by low temperature NMR point to the presence in solution of at least two main conformers, while molecular mechanics calculations describe four possible structures (Fig. 2).[24] The two conformers **A** and **B** of lowest energy present a [3434] shape with a *trans* amide group located on a 'four-bond' side. In contrast, in the two structures **C** and **D**, the amide function is accommodated in a 'three-bond' side and the conformation **D**, deriving from **C** by a NH–CO moiety rotation eliminating two corners, is considered less favourable. Similarly, X-ray studies of substituted 14-ring monolactams reveal conformations derivable from the above shapes, as described by reports on two naturally-occurring substances.[25,26]
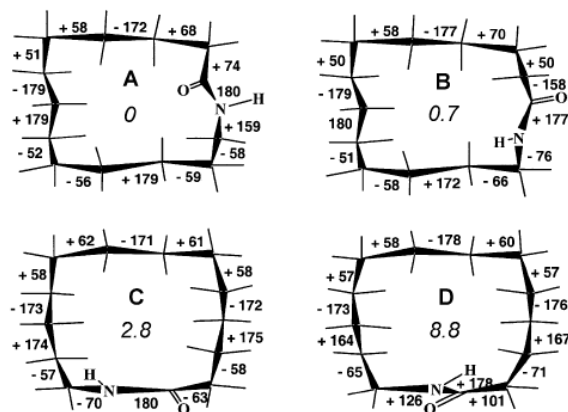
Figure 2. Top view representations of the 1-azacyclotetradecane-2-one conformers.[24] Positive and negative numbers refer to the ring torsion angles and italic numbers to the relative conformational strain energies (kJ mol^{-1}).

The X-ray diffraction of the symmetrical dilactam 1,8-di-azacyclotetradecane-2,9-dione shows a centrosymmetric ring structure with the opposite NH–CO links on the short 'sides' and adjacent angle values close to those observed in the monolactam conformer **D**.[27,28] The planes containing the amide groups are perpendicular to the average macrocyclic ring and the molecules are linked together in

---

† In Dale's convention,[4] the numbers in brackets indicate the number of C–C bonds between corner carbon atoms starting with the shortest.[4,9] Thus the [3434] conformer has two 'three-bond' sides and two 'four-bond' sides.

‡ In Snyder's designation,[9] the letters g, g′, t, corresponding to *gauche* and *trans* bonds, refer to dihedral angles varying significantly from +60°, −60°, 180°. They include the following ranges: [+45° ≤ g ≤ +105°, −45° ≤ g′ ≤ −105°, ±165° ≤ t ≤ ±180°] for cyclotetradecane[8,9] and [+50° ≤ g ≤ +126°, −50° ≤ g′ ≤ −126°, ±158° ≤ t ≤ ±180°] for 1-azacyclotetradecan-2- one (14-membered ring monolactam) (vide infra).[24] In our study, we have adopted the following convention: +20° ≤ g ≤ +116–120°, −20° ≤ g′ ≤ −116–120°, ±116–120° ≤ t ≤ ±180°.

parallel sheets by intermolecular N–H···O=C hydrogen bonds.

Concerning the 14-membered ring compounds we are interesting on, they include, besides the two symmetrical lactam functions, two infrequently encountered hybrid ketal groups with endo- and exo-cyclic oxygens that would be expected to have a strong influence on the shape of the molecules (Scheme 1). Conformational investigations were conducted by: (i) NMR spectroscopy both in solution (^{13}C and ^{1}H NMR, NOE difference) and in the solid state (^{13}C SSNMR), (ii) molecular mechanics calculations (Monte Carlo simulations) using the AMBER force field, (iii) X-ray crystallography of one macrocycle. The data obtained in this last case were compared with those deduced from the SSNMR study of the same compound. This powerful technique,[29] which offers the advantage of being easier to handle than XR diffraction, is particularly useful for studying molecular conformations that rapidly equilibrate in solution but are 'frozen out' in the crystalline state. The results obtained by the different approaches will be compared.

2. Results and discussion

Macrocyclic diketal dilactams **1–7** were prepared in two steps from β-aminoalcohols.[1] The macrocyclization strategy was based on a [1+1] cyclocondensation by *trans*-acetalization in acidic conditions of hydroxyamidoketals bearing a *trans*-amide group (Scheme 2).[1b]

Fourteen-membered macrocycles were generated under different diastereoisomeric forms depending on the chiral
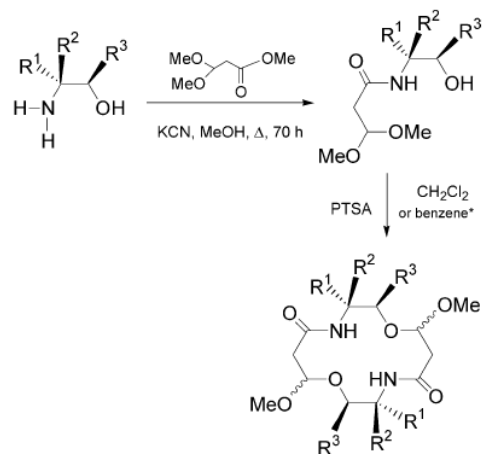
R-(-)-phenylglycinol	: R^1 = Ph; R^2 = R^3 = H	**1**
S-(+)-alaninol	: R^2 = Me; R^1 = R^3 = H	**2**
S-(+)-leucinol	: R^2 = iBu; R^1 = R^3 = H	**3**
S-(-)-phenylalaninol	: R^2 = Bn; R^1 = R^3 = H	**4**
1R,2S-(-)-norephedrine	: R^1 = H; R^2 = Me; R^3 = Ph	**5**
Aminoethanol	: R^1 = R^2 = R^3 = H	**6**
Dimethylaminoethanol	: R^1 = R^2 = Me; R^3 = H	*****7**

Scheme 2.
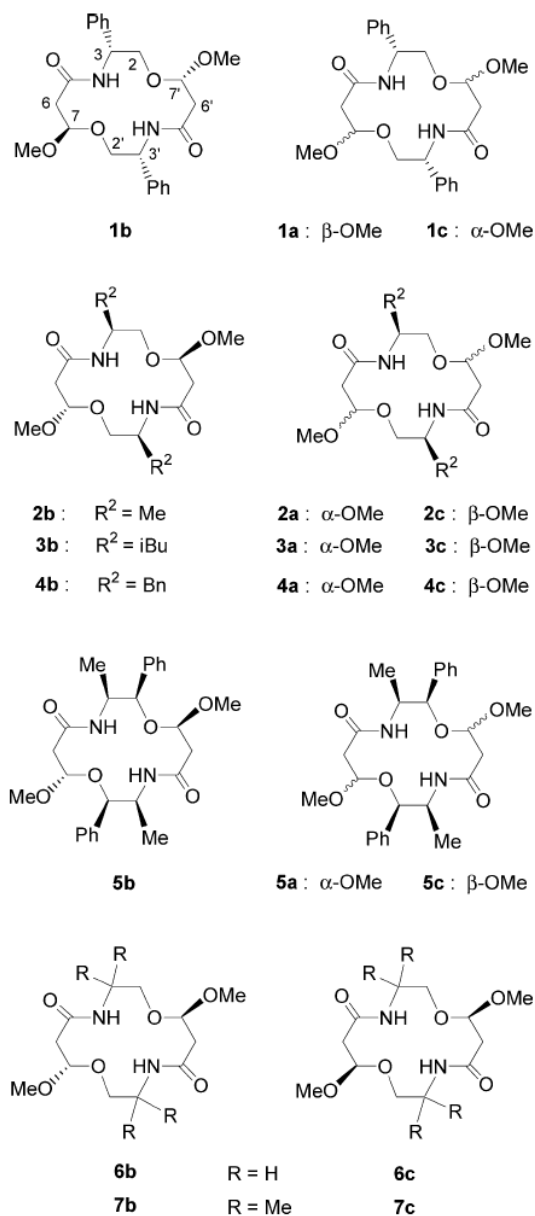
Scheme 3.

or achiral character of the starting β-aminoalcohols (Scheme 3).

The chiral series provided three diastereoisomers: an unsymmetrical isomer **b**, in which the two OMe substituents are in a *trans* configuration and two isomers **a** and **c** of C_2 symmetry, in which the two OMe groups are in a *cis* arrangement, **a** and **c** differing from each other, respectively, by the *trans* or *cis* relationship of the OMe and R groups. The achiral series led to two isomers **b** and **c** that both possessed some symmetry (center in **b**, C_2 axis in **c**).

2.1. Liquid NMR studies

Complete assignments of the liquid NMR spectra of all the macrocycles were previously reported.[1] In ^{13}C and ^{1}H

Table 1. Liquid ^{13}C NMR chemical shifts (δ in ppm) of macrocycles **1–7**

Compound	Carbon					
	C_6	C_3	OMe	C_2	C_7	CO
1a	40.0	52.5	54.5	67.6	100.1	167.9
1b chain 1	39.8	51.9	53.8	70.1	99.8	168.0
chain 1′	41.3	52.4	52.7	67.1	101.0	168.4
1c	41.2	52.5	53.2	70.5	101.2	168.4
2a	39.9	44.8	54.4	66.8	99.9	167.9
2b chain 1	39.4	44.2	54.2^a	71.0	99.7	167.8
chain 1′	41.9	44.6	52.8^a	65.7	101.3	168.3
2c	41.5	44.7	52.7	70.4	100.9	168.3
3a	39.4	46.7	54.9	64.6	99.7	167.8
3b chain 1	39.0	46.9	54.8^a	70.3	99.6	167.7
chain 1′	42.1	46.3	52.6^a	63.8	101.5	168.5
3c	41.6	47.0	52.8	69.6	101.2	168.4
4a	40.3	50.1	54.4	65.4	100.3	168.0
4b chain 1	39.9	49.6	53.8^a	68.3	100.0	167.9
chain 1′	42.1	49.6	53.7^a	65.1	101.6	168.5
4c	41.5	50.1	53.8	67.7	101.4	168.3
5a	40.6	50.1	56.5	78.0	98.6	167.9
5b chain 1	40.8	50.8	54.9	81.6	98.1	168.2
chain 1′	41.8	49.0	55.1	77.5	102.2	168.5
5c	40.9	47.9	54.6	80.7	100.0	167.8
6b	40.6	39.0	53.9	64.6	100.6	168.8
6c	41.1	39.2	53.4	66.1	100.9	169.1
7b	42.2	53.6	53.0	73.3	100.8	168.6
7c	41.9	53.5	54.2	72.8	101.3	168.5

^{a} Values which may be inverted.

NMR, chiral isomers **a** and **c** and achiral compounds **b** and **c** showed one signal for each pair of identical groups of the macrocycle, while chiral isomers **b** exhibited double signals owing to the asymmetry of the two ring chains, which could be clearly distinguished using two-dimensional NMR and INEPT long-range experiments.[1b,30] Comparison of these NMR data (chemical shifts, coupling constants, NOE difference) was used in a first approach to the conformation of the diketal dilactams studied.

2.1.1. ^{13}C NMR. Chemical shifts are collected in Table 1. For each carbon, a small variation in shielding is observed depending on the nature of the substituents R^1, R^2 and R^3 and on the stereochemistry of the OMe group. The 3-monosubstituted compounds **1–4** display the following features: (i) the ring carbons C_6, C_2, C_7 and CO appear at higher field and the OMe groups at lower field in isomers **a** than in isomers **c**, (ii) identical effects occur between chain 1 and chain 1′ of isomers **b** except for carbons C_2, which show

Table 2. Liquid NMR chemical shifts and patterns of protons H_7, H_{6A}, H_{6B} in compounds **1–7**

Compound	H_7 δ (ppm)	H_{6A} δ (ppm)	H_{6B} δ (ppm)	Pattern^a	$\Delta\nu = \nu_{6A} - \nu_{6B}$ (Hz)
1a	4.77	2.80	2.58	3dd	89.0
1c	4.78	2.64	2.62	ABX	5.0
1b chain 1	4.77	2.86	2.56	3dd	120.3
chain 1′	4.82	2.60	2.59	ABX	3.7
2a	4.77	2.74	2.55	3dd	98.0
2c	4.69	2.58	2.54	ABX	17.4
2b chain 1	4.74	2.77	2.50	3dd	108.0
chain 1′	4.75	2.56	2.53	ABX	11.6
3a	4.78	2.75	2.54	3dd	87.0
3c	4.65	2.55	2.53	ABX	10.9
3b chain 1	4.74	2.79	2.50	3dd	114.0
chain 1′	4.73	2.55	2.51	ABX	14.3
4a	4.64	2.70	2.47	3dd	92.0
4c	4.63	2.55	2.55	ABX ≈ d+t	0
4b chain 1	4.63	2.76	2.47	3dd	115.0
chain 1′	4.65	2.52	2.45	ABX	28.3
5a	4.55	2.78	2.76	ABX	6.1
5c	4.95	2.77	2.65	ABX ≈ 3dd	47.6
5b chain 1	4.49	2.83	2.65	3dd	72.6
chain 1′	4.89	2.77	2.65	ABX ≈ 3dd	49.8
6b	4.77	2.66	2.56	ABX ≈ 3dd	43.1
6c	4.69	2.63	2.59	ABX	34.5
7b	4.70	2.55	2.45	ABX	39.8
7c	4.70	2.60	2.49	ABX ≈ 3dd	44.1

^{a} ABX system for $\Delta\nu < 5 \times J_{6A-6B}$ with $J_{6A-6B} = 13.4$–16.1 Hz.

Table 3. Coupling constants (J in Hz) of compounds 1-7 in liquid ^{1}H NMR

Compound[a]	$|J_{3\text{-}2A}|$	$|J_{3\text{-}2B}|$	$|J_{7\text{-}6A}|$	$|J_{7\text{-}6B}|$
1a	3.2	4.4	7.2	2.1
1b chain 1	3.1	3.3	8.4	1.7
chain 1$'$	3.2	5.5	1.6	9.0
1c	4.9	3.3	9.7	0.3
2a	3.2	4.3	7.5	2.1
2b chain 1	2.1	2.7	8.6	1.8
chain 1$'$	2.7	4.3	1.9	9.3
2c	3.2	2.9	8.5	2.2
3a	2.8	2.8	7.9	2.2
3b chain 1	1.4	2.7	8.7	1.7
chain 1$'$	2.6	0.5	2.1	9.3
3c	2.6	2.6	8.3	1.8
4a	3.0	4.0	6.6	2.0
4b chain 1	2.5	3.0	7.9	1.8
chain 1$'$	3.0	4.8	2.1	8.7
4c	3.2	3.0	4.7	4.7
5a	2.7		3.6	1.2
5b chain 1	2.0		6.1	0.5
chain 1$'$	3.0		6.7	1.8
5c	2.9		2.6	5.2
6b[b]	3.0	6.8	8.3	2.0
	6.0	2.6		
6c[b]	4.5	2.1	8.2	1.8
	2.9	9.2		
7b	-	-	8.3	1.9
7c	-	-	7.1	2.2

[a] For all compounds $|J_{2A\text{–}2B}| = 8.8\text{–}10.0$ Hz; $\Delta\nu = \nu_{2A} - \nu_{2B} = 76\text{–}184$ Hz.
[b] First line: $J_{3A\text{–}2X}$; second line: $J_{3B\text{–}2X}$.

an upfield shift in chain 1$'$, (iii) in isomers **b**, chemical shift values of carbons C_6, C_7, CO and OCH_3 (chain 1) are nearly identical to those of isomers **a**, while carbon δ values of chain 1$'$ are close to those of isomers **c**.

These observations suggest that in each series, the variations in shielding depend essentially on the stereochemistry of the OMe group. Thus a *trans* relationship between OMe and the R^1 or R^2 substituents as it exists in isomers **a** and in chain 1 of isomers **b** induces shielding of the nearest carbons C_7, C_6, C_5 and $C_{2'}$ while a *cis* relationship as it exists in isomers **c** and in chain 1$'$ of isomers **b** causes deshielding of carbons $C_{7'}$, $C_{6'}$, $C_{5'}$ and C_2.

2.1.2. ^{1}H NMR. Firstly, a careful analysis of the splitting of H_{6A} and H_{6B} due to coupling with the H_7 proton (Table 2) reveals that in 3-monosubstituted compounds **1–4**, these hydrogens appear as a doublet of doublet in each isomer **a** and as an ABX system in each isomer **c**. An identical splitting difference of protons H_{6A} and H_{6B} is also observed between the two chains of isomers **b**. In fact, H_{6A} hydrogens in **1a–4a** and **1b–4b** (chain 1) are curiously deshielded ($\Delta\delta \approx +0.16 - +0.30$ ppm) compared with all the other H_6 protons. This effect may be due to a greater proximity of H_{6A} and the OMe oxygen lone pair in these cases. This hypothesis is supported below. In the norephedrine series in which the macrocycles have two substituents ($R^2 = $Me and $R^3 = $Ph), the same observations can be made regarding the two chains of compound **5b**. In contrast, and surprisingly, an inversion occurs in the splitting of **5a** and **5c** that is a real ABX system for **5a** and an ABX system close to 3dd ($\Delta\nu \approx 3 \times J_{6A\text{-}6B}$) for **5c**. This last pattern is also present in achiral compounds **6b** and **7c**.

Secondly, examination of coupling constants of H_3 and H_7

with their vicinal hydrogens provides information on their position in the ring (Table 3). Thus, in all the compounds, H_3 hydrogens whose both coupling constants have small values ($J_{3\text{-}2A} = 1.4\text{–}4.9$ and $J_{3\text{-}2B} = 0.5\text{–}5.5$ Hz) probably occupy an equatorial position bisecting the dihedral angle H_{2A}–C–H_{2B}. Similarly, H_7 protons, which in most compounds have widely different J values ($J_{7\text{-}6ax} = 4.7\text{–}9.7$, $J_{7\text{-}6eq} = 0.3\text{–}4.7$ Hz), very likely occupy an axial position with axial–axial and axial–equatorial coupling constants, respectively. One exception is, however, observed for **5a** in which H_7 protons show closer J values (3.6 and 1.2 Hz) corresponding to a pseudo-axial or equatorial position of H_7 due to a modification of the ring shape.

Thirdly, a complementary study by the ^{1}H–^{1}H nuclear Overhauser effect (NOE) was made on compounds **1c**, **2c**, **6c** and **7c** to obtain further information on the spatial interactions. Irradiation of H_7 produces nuclear Overhauser enhancements on: (i) H_{6B} for which a differentiated effect with regard to H_{6A} is clearly visible on compounds **6c** and **7c** but not on compounds **1c** and **2c**, the $\Delta\nu$ values being

Table 4. (a) In normal characters: nuclear Overhauser effects (%) observed on protons H_x by irradiation of H_7 for compounds **1c**, **2c**, **6c**, **7c**; (b) in italic characters: interatomic distances $d_{H_7\text{–}H_x}$ (Å) measured by molecular modeling

Compound	Proton		
	H_{2A}	H_{2B}	H_{6B}
1c	0.0%	3.6%	5.0%
	2.93	*2.41*	*2.52*
2c	1.0%	3.7%	4.2%
	2.89	*2.42*	*2.52*
6c	0.5%	4.0%	3.1%
	2.92	*2.38*	*2.53*
7c	0%	3.9%	5.2%
	2.91	*2.36*	*2.53*

large in the first case and small in the second case (Table 2), (ii) H_{2B} whereas no appreciable effect is observed on H_{2A} (Table 4). This last result points to a partial strain in the assumed high flexibility of the macrocycles which would produce an effect on both H_2 protons. In contrast, the observed NOE indicates that H_7 must be *cis* to H_{2B} and *trans* to H_{2A}. Taking into account the axial position of H_7 and the equatorial position of H_3 in **1c** and **2c** (see above), these results identify H_{2A} as H_{2eq} and H_{2B} as H_{2ax} in all isomers **c**, in particular in the 3-disubstituted compound **7c**, for which J_{3-2} coupling constants are not available.

2.2. Molecular modeling

The Monte-Carlo calculations indicate a certain flexibility of these macrocyclic ligands, for which ten conformations are generally observed within 4–13 kJ mol^{-1} of the global minimum (Supplementary material SM). However, in around 60% of cases (11/19), a greater energy difference is observed between the first two conformers than between the five following ones taken two by two ($\Delta E_{2-1} > \Delta E_{3-2}$ or ΔE_{4-3} or ΔE_{5-4}). Hence, because a detailed comparison of all the conformers would have been tedious and difficult, the modeling study was conducted, for most of the compounds, on the first conformer of lowest energy, and only exceptionally on the following ones.

The calculated H–H dihedral angles (SM) for conformer **1** of most of the chiral compounds (**1a–c**, **2a–c**, **3b**, **4c**, **5a,c**) point to: (i) an equatorial position of H_3 bisecting the angle H_{2ax}–C–H_{2eq} ($\theta_{H_3,H_{2ax}} = 33–63°$ and $\theta_{H_3,H_{2eq}} = 54–85°$) and corresponding to an axial position of the 3,3'-R groups (α-axial in **1**, β-axial in **2–5**) and to an equatorial position of the 2,2'-Ph substituents in macrocycles **5a** and **5c**, (ii) an axial position of H_7 ($\theta_{H_7,H_{6ax}} = 168–180°$) corresponding to an energetically favourable equatorial position of the α or β-OMe groups. These observations, not made in the first conformer of **3a** and **4a**, are consistent, however, with the second conformer. These results agree with the above ^{1}H NMR data: equatorial and axial characters of H_3 and H_7, respectively. The preferential 3-R substituent axial position and the preferential OMe group equatorial situation may produce a partial strain in these otherwise flexible compounds, as suggested by the NOE results (vide supra). Two exceptions are, however, to be noted for the chain 1' of macrocycles **4b** and **5b**, in which $H_{3'}$ or $H_{7'}$ or both protons occupy an opposite situation on the first conformers, while the above conformation ($H_{3'eq}$ and $H_{7'ax}$) occurs only on conformer 5 of **4b** and on conformer 8 of **5b**. In the NMR spectrum of **4b**, the $J_{3'-2'B}$ value (4.8 Hz), which corresponds to the maximum of the observed J_{3-2} values, is consistent with an equilibrium between the conformers of lowest energy. Also, the assumed equatorial position of H_7 in compound **5a** (see above) is confirmed for the chain 1' of the second conformer ($\theta_{H_{7'},H_{6'ax}} = 55°$ and $\theta_{H_{7'},H_{6'eq}} = 62°$).

Measurements of the H_6–OMe interatomic distances indicate a shorter $d_{H_{6ax}-OMe}$ for compounds **a** and **b** (chain 1) (2.69–2.76 Å) than for compounds **c** and **b** (chain 1') (2.80–2.87 Å) (SM). These indications are evidenced in most of conformers 1 (**1a–c**, **2a–c**, **3b–c**, **4c**, **5a,c**), in conformer 2 of **3a** and **4a**, in conformer 5 of **4b** and in conformer 8 of **5b**. They are consistent with the deshielding

observed for H_{6A} in compounds **a** and **b** (chain 1) (see above) that is to say in the chain in which the 7-OMe group is in a *trans* relationship with the 3-R substituent. C–C dihedral angles of the 19 macrocycles are given in Table 5. All exhibit invariable transoid conformations along the two bonds C_3–N_4–CO–C_6 corresponding to the amide links (torsions: 172–180°) and the two bonds $C_{7'}$–O_1–C_2–C_3 (torsions: 121–180°), and *gauche* conformations along the bonds O_1–C_2–C_3–N_4 (torsions: 34–72°) and C_5–C_6–C_7–$O_{1'}$ (torsions: 50–75°). In contrast, the values of the C_2–C_3–N_4–C_5, N_4–C_5–C_6–C_7 and C_6–C_7–$O_{1'}$–$C_{2'}$ angles range from 22 to 180° and correspond to *gauche* or *trans* (*anti*) conformations depending on the macrocycle stereochemistry and the nature of the substituents.

In the achiral compounds, structures of the [3434]-type are observed for the symmetry center macrocycles **6b** and **7b** (structure Ib) in which the *trans*-OMe groups are accommodated in the two opposite corners C_7, $C_{7'}$, while the C_3, $C_{3'}$ carbons form the other two corners (Fig. 3). The O_1, $O_{1'}$ atoms, located on the 'three-bond' sides, point inwards into the ring. The *trans*-amide functions, situated on the 'four-bond' sides, are set perpendicular to the macrocyclic plane and display the conformationally more stable opposite orientation.[27] The rectangular diamond-lattice structure is magnified in compound **7b** (N_4–C_5–C_6–C_7, $N_{4'}$–$C_{5'}$–$C_{6'}$–$C_{7'}$ dihedral angles $= \pm 145°$ in **6b**, $\pm 172°$ in **7b**) by the presence in C_3, $C_{3'}$ of *gem*-dimethyl groups (see above).[11,12] In the *cis*-OMe isomers **6c** and **7c** (structure IIc), the potential rectangular shape is distorted compared with **6b** and **7b** by a $\approx 180°$ rotation of one NH-CO group, eliminating the C_7, $C_{7'}$ corners and causing the appearance in C_6 and $C_{6'}$ of g'g sequences accompanied by an increase to 95 or 119° of one of the corresponding dihedral angles as indicated above for some conformers of cyclotetradecane.[8] The NH–CO links are still perpendicular to the macrocycle, but in this case they are located on the pseudo three-bond sides and oriented in the same direction, in agreement with a C_2 symmetry, while the O_1 and $O_{1'}$ atoms, still pointing into the ring, now occupy the middle position of the four-bond side (Fig. 3).

In the chiral compounds **1–5**, the conformation of the molecules is modified, compared with the above shapes, by a 90° rotation of one or both NH–CO links, which take a position parallel to the average macrocycle plane, with the C=O and N–H bonds directed outwards from and inwards into the ring respectively. This arrangement allows the formation of intramolecular hydrogen bonds between the NH hydrogens and the endocyclic ketal oxygens of the other chain, which are invariably oriented inwards into the ring (Fig. 3). Thus while most of *trans* compounds **b** (**2b–5b**), exhibit only one N_4–H···$O_{1'}$ bond, *cis* macrocycles **a** and **c** are characterized in most cases [**1a–3a**, **1c–3c**, **4a** (conformer 2), **4c** (conformer 5), **5a**, **5c**] by the presence of two hydrogen bonds N_4–H···$O_{1'}$ and $N_{4'}$–H···O_1 consistent with a C_2 symmetry (SM).

All these molecules show gg' or g'g arrangements for C_6, $C_{6'}$ with N_4–C_5–C_6–C_7 and C_5–C_6–C_7–$O_{1'}$ angles ranging from ± 22 to $\pm 122°$ (Table 5). They differ essentially in the values of the dihedral angles C_2–C_3–N_4–C_5 and

Table 5. C–C torsional angles ϕ (°) for macrocycles 1–7 (+20°<g<+116–126°; −20°<g'<−116–126°; ±116–126°<t<±180°

Macrocycle	ϕ														Nomemclature	Structure
	C7'–O1–C2–C3	O1–C2–C3–N4	C2–C3–N4–C5	C3–N4–C5–C6	N4–C5–C6–C7	C5–C6–C7–O1'	C6–C7–O1'–C2'	C7–O1'–C2'–C3'	O1'–C2'–C3'–N4'	C2'–C3'–N4'–C5'	C3'–N4'–C5'–C6'	N4'–C5'–C6'–C7'	C5'–C6'–C7'–O1	C6'–C7'–O1–C2		
1a conf 1	+153	+34	+152	−172	−62	+59	+177	+153	+34	+152	−172	−61	+59	+177	tgttg'gttgttg'gt	Enan Ia[a]
2a conf 1	−174	−52	−148	+179	+29	−62	−69	−174	−52	−148	+180	+29	−62	−69	tg'ttgg'g'tg'ttgg'g'	IIa
3a conf 1	+171	−53	−131	+177	+40	−69	+170	+172	+51	−160	−178	−49	+55	+167	tg'ttgg'ttgttg'gt	I'a
3a conf 2	−179	−54	−148	−179	+36	−64	−71	−174	−57	−130	−179	+22	−61	−72	tg'ttgg'g'tg'ttgg'g'	IIa
4a conf 1	−174	−48	−150	+175	+49	−69	+177	+174	+63	−165	+177	−66	+54	+169	tg'ttgg'ttgttg'gt	I'a
4a conf 2	+168	−62	−106	−178	+28	−64	−80	+168	−60	−109	+179	+32	−65	−80	tg'tgg'g'tg'g'tgg'g'	IIIa
5a conf 1	+138	−61	−80	+180	+40	−64	−78	+138	−61	−80	+180	+40	−64	−78	tg'g'tgg'g'tg'g'tgg'g'	IIIa
5a conf 2	+162	−49	−135	+175	+45	−68	+177	+167	+46	−166	−179	−44	+59	+166	tg'ttgg'ttgttg'gt	I'a
1b conf 1	−176	+49	+152	+178	−47	+66	+70	+170	+47	+156	+176	+58	−68	+177	tgttg'ggtgttg't	Enan IIb[a]
2b conf 1	+179	−54	−143	+180	+43	−66	−68	−168	−50	−147	−179	−65	+68	−174	tg'ttgg'g'tg'ttg'gt	IIb
3b conf 1	+177	−55	−143	−180	+48	−68	−68	−166	−53	−128	−179	−78	+68	−173	tg'ttgg'g'tg'ttg'gt	IIb
4b conf 1	+172	−60	−154	+177	+52	−69	+176	+174	+64	−159	+180	−76	+69	−180	tg'ttgg'ttgttg'gt	IIIb
4b conf 5	+166	−60	−99	−180	+28	−63	−76	+177	−62	−140	−172	−47	+67	+179	tg'ttgg'ttgg'tg'gt	IVb
5b conf 1	+143	−52	−151	+175	+62	−73	+177	+158	+59	−93	+179	−122	+70	−171	tg'ttgg'ttgg'tg'gt[c]	Vb[c]
5b conf 8	+116	−52	−74	+175	+47	−64	−79	+142	−72	−83	−170	−45	+68	−171	tg'g'tgg'g'tg'g'tg'gt[c]	VIb[c]
6b conf 1	+179	+60	+83	−179	+145	−60	−72	−180	−60	−83	+179	−145	+60	+72	tggttg'g'tg'g'tl'gg	Ib [3434]
7b conf 1	−172	+55	+61	−178	+172	−62	−75	+172	−55	−61	+178	−172	+62	+75	tggttg'g'tg'g'ttgg	Ib [3434]
1c conf 1	+176	+51	+155	+178	+47	−71	+175	+176	+51	+155	+178	+47	−71	+175	tgttg'ttgttgg't	Enan Ic[a]
1c XR[b]	−84	−62	+143	−179	+93	−70	+176	−84	−62	+143	−179	+93	−70	+176	g'g'ttgg'tg'g'ttgg't	
2c conf 1	−174	−54	−147	−179	−50	+71	−174	−174	−54	−147	−179	−50	+71	−174	tg'ttg'gttg'ttg'gt	Ic
3c conf 1	−175	−58	−128	−178	−59	+71	−175	−175	−58	−128	−178	−59	+71	−175	tg'ttg'gttg'ttg'gt	Ic
4c conf 1	+170	−61	−127	−176	−45	+70	+179	−179	−64	−86	+178	−82	+73	−179	tg'ttg'gttg'g'tg'gt	IIIc
4c conf 5	+172	−62	−134	−175	−44	+69	−179	+180	−64	−116	−179	−58	+72	−180	tg'ttg'gttg'ttg'gt[c]	Ic[c]
5c conf 1	+121	−60	−78	−177	−41	+68	−176	+121	−60	−78	−177	−41	+68	−176	tg'g'tg'gttg'g'tg'gt[c]	IIc[c]
6c conf 1	−178	−59	−80	−180	−95	+72	−172	−178	−59	−79	−180	−95	+72	−172	tg'g'tg'gttg'g'tg'gt	IIc
7c conf 1	−179	−54	−59	+179	−119	+72	−172	−179	−54	−59	+179	−119	+72	−172	tg'g'tg'gttg'g'tg'gt	IIc

[a] Enan=Enantiomer of structure.
[b] X-ray angle data.
[c] Hybride structure for: 5b conformer 1: tg'ttgg'ttgg'tg'gt (Vb) or tg'ttgg'ttgg'ttgt due to one hybride angle of 122°; 5b conformer 8: tg'g'tgg'g'tg'g'tg'gt (VIb) or gg'g'tgg'g'tg'g'tg'gt due to one hybride angle of 116°; 4c conformer 5: tg'ttg'gttg'ttg'gt (Ic) or tg'ttg'gttg'g'tg'gt (IIIc) due to one hybride angle of 116°; 5c conformer 1: tg'g'tg'gttg'g'tg'gt (IIc) or gg'g'tg'gtgg'g'tg'gt due to two hybride angles of 121°.

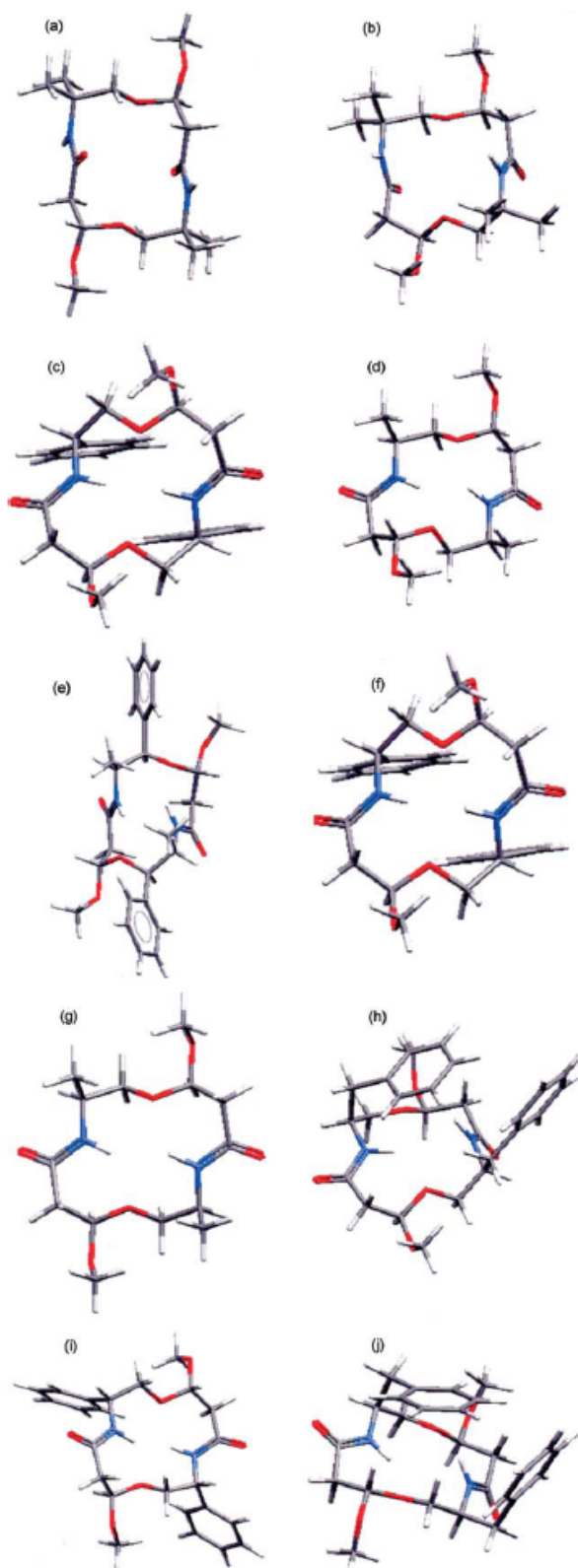C_6–C_7–$O_{1'}$–$C_{2'}$ which can correspond to either a *trans* or a *gauche* conformation.

Thus chiral macrocycles **a** present four different structures: (i) structure Ia: tg′ttgg′ttg′ttgg′t (enantiomer of **1a**)[§] and structure I′a: tg′ttgg′ttgttg′gt (**3a** conformer 1, **4a** conformer 1, **5a** conformer 2) neither of which have a corner, and which present an identical chain 1, but which differ in the sign of the chain 1′ *gauche* angles, causing a loss of symmetry in I′a, (ii) structure IIa: tg′ttgg′g′tg′ttgg′g′ (**2a** conformer 1, **3a** conformer 2) characterized by the presence of corners at C_7, $C_{7'}$, (iii) structure IIIa: tg′g′tgg′g′tg′g′tgg′g′ (**4a** conformer 2, **5a** conformer 1) which has corners at C_3, $C_{3'}$ and C_7, $C_{7'}$.

Chiral compounds **c** present three different structures: (i) structure Ic: tg′ttg′gttg′ttg′gt, the most frequently observed (enantiomer of **1c**,[§] **2c**, **3c**, **4c** conformer 5), which has no corner; (ii) structure IIc: tg′g′tg′gttg′g′tg′gt (**5c** conformer 1) characterized by the presence of two corners at C_3, $C_{3'}$ as previously observed in achiral macrocycles **6c** and **7c**; the three compounds differ essentially in some lower dihedral angle values in **5c**: N_4-C_5−C_6-$C_{7'}$, $N_{4'}$-$C_{5'}$−$C_{6'}$-$C_{7'}$ (95 and 119° in **6c** and **7c**, 41° in **5c**) and $C_{7'}$–O_1–C_2–C_3, C_7–O_1–$C_{2'}$–$C_{3'}$ (178–179° in **6c** and **7c**, 121° in **5c** (limit value between *trans* and *gauche* conformations)]; (iii) structure IIIc: tg′ttg′gttg′g′tg′gt (**4c** conformers 1–4), which has a single corner at $C_{3'}$ with no symmetry, and which is composed of chain 1 of Ic and chain 1′ of IIc. Structures Ic, IIc and IIIc differ in the values of the four angles C_2-C_3–N_4-C_5, $C_{2'}$-$C_{3'}$–$N_{4'}$-$C_{5'}$ and C_6-C_7—O_1-$C_{2'}$, $C_{6'}$-$C_{7'}$-O_1-C_2, as seen above.

Chiral macrocycles **b**, whose chain 1 possesses the stereochemistry of compounds **a** and chain 1′ the stereochemistry of compounds **c**, can adopt various combinations between structures Ia–IIIa and Ic–IIIc to give five different conformations IIb–VIb.

The representation of compounds with identical stereochemistry, for example macrocycles **c**, along a horizontal C_7-$C_{7'}$ axis, with the OMe groups at each extremity, allows an interesting comparison of the global shape of the skeletons in function of the nature of the substituent (Fig. 4). Thus, all molecules of structure Ic [enantiomer of **1c**, **2c**, **3c** (conformers 1) and **4c** (conformer 5)] adopt a nearly identical pseudo-planar shape, while molecules with structure IIc show a convex form, slight in **6c** and **7c**, and marked in **5c**.

2.3. X-ray crystallography

The previously determined crystal structure[1a] of macrocycle **1c** presents Ph and OMe substituents in an equatorial position. It shows a g′g′ttgg′tg′g′ttgg′t conformation close to that observed for **6c** and **7c** in molecular modeling (see

Figure 3. Top view representations of some diketal dilactam macrocycles (conformer 1) by molecular modeling: (a) **7b**: structure Ib, (b) **7c**: structure IIc, (c) **1a**: enantiomer of structure Ia, (d) **2a**: structure IIa, (e) **5a**: structure IIIa, (f) **1c**: enantiomer of structure Ic, (g) **2c**: structure Ic, (h) **4c**: structure IIIc, (i) **1b**: enantiomer of structure IIb, (j) **4b**: structure IIIb.

[§] Macrocycle **1a** with an *R* stereochemistry at C-3 and C-3′ corresponds to a tgttg′gttgttg′gt structure. To establish comparison with the 3-*S* compounds **2a**, **3a**, **4a** and **5a**, we have to consider the 3-*S* enantiomer of **1a**, the designation of which would be tg′ttgg′ttg′ttgg′t. Identical modifications have to be made for **1b** (tgttg′ggtgttgg′t) and **1c** (tgttg′ttgttgg′t), enantiomers of which would have tg′ttgg′g′tg′tg′ttg′gt and tg′ttg′gttg′ttg′gt structures, respectively.

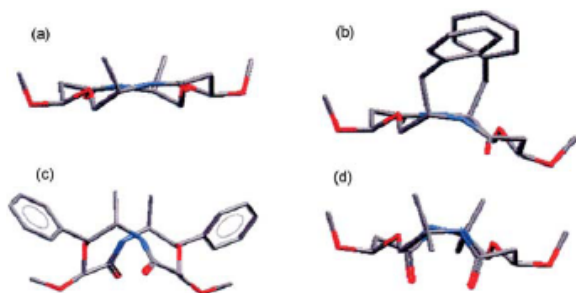**Figure 4.** Representation by molecular modeling of some macrocycles c with a horizontal C_7–$C_{7'}$ axis: (a) **2c** conformer 1: structure Ic, (b) **4c** conformer 5: structure Ic, (c) **5c** conformer 1: structure IIc, (d) **7c** conformer 1: structure IIc.

above) and characterized by a C_2 symmetry, gg' sequences at C_6, $C_{6'}$ and corners at C_2, $C_{2'}$ instead of C_3, $C_{3'}$, consequent to a shift of the pseudo three- and four-bond sides (Table 5). Besides, in comparison with **1c** (conformer 1), transoid conformations are also observed along the bonds C_2–C_3–N_4–C_5, C_6–C_7–$O_{1'}$–$C_{2'}$ and of course along the amide links, but in the crystal, the two $C_{7'}$–O_1–C_2–C_3
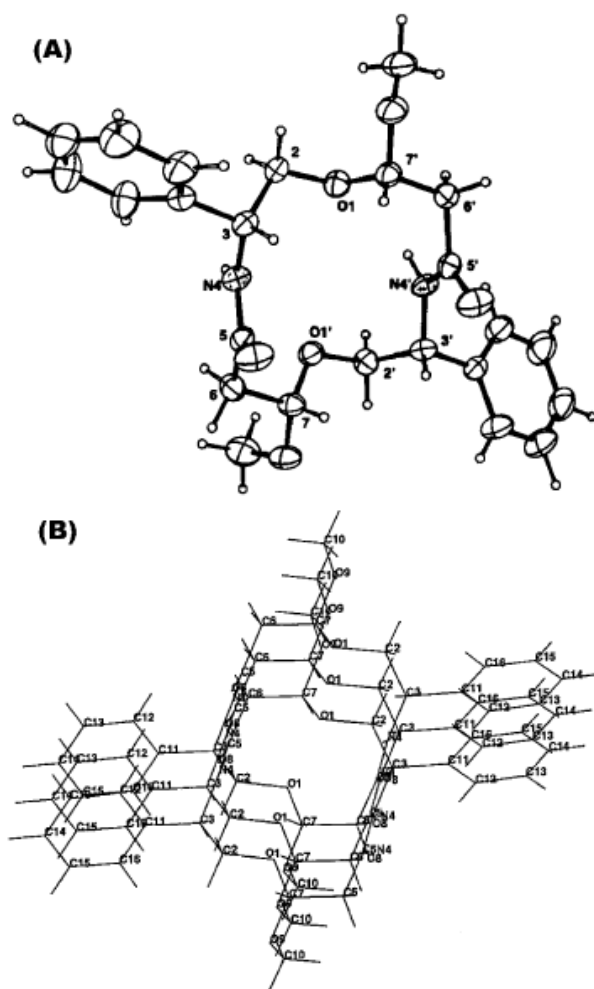

Figure 5. Phenyl macrocycle **1c**: (A) X-ray structure;[1a] (B) Stacking of the molecules in parallel layers.[1a]

bonds correspond to a *gauche* conformation. Also, the O_1, $O_{1'}$ atoms still point into the ring but the NH–CO links, located on the pseudo four-bond sides are now perpendicular to the macrocyclic plane and oriented in the same direction (Fig. 5). This arrangement in the crystal allows, the formation of N–H···O=C intermolecular hydrogen bonds (2.95 Å) that link the molecules together into sheets parallel to the binary axis,[1a] while π–π stacking interactions between the phenyl groups may also reinforce the cohesion of the structure.

2.4. Solid state NMR analysis

When no suitable crystals are available for an X-ray study, structural information concerning the solid state can be obtained by SSNMR. This technique, which unlike liquid NMR does not reflect an averaged conformation, permits the analysis of conformational constraints and polymorphic forms. Associated with magic angle spinning, the most common NMR experiment designed for this purpose is certainly the cross-polarization pulse scheme (CP-MAS), which allows a marked sensitivity enhancement and reduced acquisition time. Thus SSNMR spectra were first recorded for compounds **1a**, **1b** and **1c** to evaluate the effect of the relative positions of the 3,3'-R substituents (Ph in the present case) and the 7,7'–OMe groups on the ring conformation. Compounds **2c**, **3c**, **4c**, **6b** and **6c** were then analyzed to study the effect of the nature of the 3,3'-R substituent. Unfortunately, no suitable solid for NMR analysis was obtained for macrocycles **5**.

The solid state NMR spectra of the three phenyl isomers **1a–c** were recorded in the same conditions and compared with the corresponding liquid state ^{13}C NMR spectra, and for **1c** to its X-ray diffraction data.[1a] In agreement with the liquid state ^{13}C NMR spectra, isomers **a** and **c** show one signal for each pair of identical groups of the macrocycle, while isomer **b** exhibits double signals (Table 6).

Concerning isomer **1c**, the presence of a high symmetry is readily apparent in its ^{13}C CP-MAS spectrum which shows 10 signals for the twenty carbons (SM). Several very interesting singularities can be noted in comparison with the ^{13}C liquid spectrum: (i) deshielding ($\Delta\delta + 1.5$ ppm) of the CO peak, which confirms the presence of intermolecular C=O···HN hydrogen bonds[31,32] as observed by X-ray diffraction analysis; (ii) shielding of the methoxy groups ($\Delta\delta -6.4$ ppm), which can be distinguished from C_3 carbons by dipolar dephasing experiments[¶,33] and by comparison of the signal shape (sharp singlet for OMe and broadened singlet for C_3 due to a quadrupolar coupling with the a ^{14}N atom);[34] (iii) shielding of C_7 ($\Delta\delta -6.2$ ppm) and C_3 ($\Delta\delta -1.2$ ppm) carbon signals due to a γ-*gauche* effect known to give substantially shielded ^{13}C resonances[35–37] and resulting from $C_{7'}$–O_1–C_2–C_3 *gauche* conformations, present in the solid state (torsions: 84° from X-ray data) and not in the liquid state (torsions: 176° from molecular modeling data). Complementary NMR experiments were conducted on this isomer by varying the

---

¶ Dipolar dephasing induces fast dephasing of protonated carbon signals (CH, CH$_2$) except for those of CH$_3$ groups which have a higher 'mobility'.

Table 6. SSNMR ^{13}C chemical shifts (δ in ppm) of compounds 1a-c, 2c-4c and 6b,c. Values in *italic* correspond to chemical shift differences between solid and liquid states ($\Delta\delta = \delta_{sol.} - \delta_{liq.}$)

Compound	Carbon					
	C_6	C_3	$O-CH_3$	C_2	C_7	$C=O$
1a	43.2	54.0[a]	54.0[a]	74.7	102.6	169.4
	+3.2	*+1.5*	*−0.5*	*+7.1*	*+2.5*	*+1.5*
1b chain 1	43.2[a]	54.0[a]	54.0[a]	74.7	103.5	169.4[a]
	+3.4	*+2.1*	*+0.2*	*+4.6*	*+3.7*	*+1.4*
chain 1'	43.2[a]	51.1	46.8	67.1	94.6	169.4[a]
	+1.9	*−1.3*	*−5.9*	*0.0*	*−6.4*	*−1.0*
1c	42.9	51.3	46.8	67.3	94.9	169.9
	+1.7	*−1.2*	*−6.4*	*−3.2*	*−6.3*	*+1.5*
2c	40.1	46.1/45.4[b]	48.7	71.1	100.9	171.0/170.2[b]
	−1.4	*+1.4/+0.7*	*−4.0*	*+0.7*	*0.0*	*+2.7/+1.9*
3c polymorph 1[c]	42.0	47.9	54.5	72.3	103.5	169.0
	+0.4	*+0.9*	*+1.7*	*+2.7*	*+2.3*	*+0.6*
polymorph 2[c]	42.3	47.8	54.0/54.4	69.9/70.4	103.1	168.6
	+0.7	*+0.8*	*+1.2/+1.6*	*+0.3/+0.8*	*+1.9*	*+0.2*
4c[d]	40.9/43.1	51.8[a]	55.1/56.8	64.4/71.5	100.5/104.9	169.1[a]
	−0.6/+1.6	*+1.7*	*+1.3/+3.0*	*−3.3/+3.8*	*−0.9/+3.5*	*+0.8*
6b	39.2	37.6	56.8	61.0	102.2	168.5
	−1.4	*−1.4*	*+2.9*	*−3.6*	*+1.6*	*−0.3*
6c	40.7	40.1	47.9	64.4	100.6	170.9
	−0.4	*+0.9*	*−5.5*	*−1.7*	*−0.3*	*+1.8*

[a] Values corresponding to unresolved and/or broad signals.
[b] Asymmetric doublet resulting from the quadrupolar moment of ^{14}N.
[c] Polymorphs 1 and 2 present the same solution spectrum.
[d] Compound 4c does not show any difference between the two chains in liquid NMR.

temperature in the solid and liquid states. The aim of these studies was to explore potential conformational changes by: (i) increasing the temperature in the solid state to enhance the flexibility of the ring and ultimately approach $C_{7'}-O_1-C_2-C_3$, $C_7-O_{1'}-C_{2'}-C_{3'}$ *trans* conformations, (ii) decreasing the temperature in the liquid state to obtain a more constrained conformation. At 130 °C (maximum temperature technically available), no change was detected in the SSNMR spectra. In contrast, at −80 °C (minimum temperature available in CD_2Cl_2)$^{\|}$ all resonances, except the CO one, were shielded from about 0.6–1.0 ppm, in particular the C_7 resonance ($\Delta\delta$ −0.8 ppm), shielding of which is consistent with possible *gauche* conformations at low temperature in the liquid state.

As noted for isomer **1c**, the symmetry of isomer **1a** is conserved in the solid state NMR spectrum. Compared with the liquid NMR spectrum, the deshielding of the CO carbon ($\Delta\delta$ +1.5 ppm) underlines again the presence of intermolecular CO···HN hydrogen bonds. Besides, the C_7 shift variation ($\Delta\delta$ +2.5 ppm) indicates that no γ-*gauche* effect occurs in the solid state of this compound.

Concerning isomer **1b**, its ^{13}C SSNMR spectrum, which should exhibit two signals for each pair of identical groups, is characterized by 11 resolved lines: in fact, only the OMe, C_3, C_2 and C_7 carbons are split. Intermolecular CO···HN hydrogen bonds are present once more as shown by the shift of the CO carbons ($\Delta\delta$ +1.4 and +1.0 ppm). Besides, as previously observed in the liquid NMR spectrum, the ^{13}C chemical shifts of chain 1 are nearly identical to those of **1a**, and the δ values of chain 1' are close to those of **1c** (Table 6). These results indicate that a *trans* relationship between

the 3-phenyl substituents and the OMe groups (as occurs in isomer **a**) implies *trans* or *anti* $C_{7'}-O_1-C_2-C_3$ conformations, while a *cis* relationship (as occurs in isomer **c**) implies *gauche* $C_{7'}-O_1-C_2-C_3$ conformations in the solid state in contrast with the *anti* conformations observed in the liquid phase.

Consequently if a positive difference in chemical shifts between the solid and liquid spectra ($\Delta\delta = \delta_{solid} - \delta_{liquid} \geq 0$) is observed for the C_7 carbon, a *trans* conformation may be expected. In contrast, if $\Delta\delta < 0$, a degree of conformational constraint, such as a *gauche* conformation, may be expected. The results obtained for the other compounds will be discussed on this basis.

The SSNMR spectrum of compound **2c** which presents seven resonances for 14 carbons, indicates that the symmetry is also preserved in the solid phase (Table 6). The CO downfield effect ($\Delta\delta = +1.9 - +2.7$ ppm) may be due, as seen above, to the presence of intermolecular CO··· HN hydrogen bonds. Besides, the C_7 chemical shift variation ($\Delta\delta$ 0 ppm) is broadly indicative of a globally non-constrained conformation for **2c** in the solid state. Thus, the simple presence of a methyl group in the C_3 position appears insufficient to produce a constrained conformation.

The symmetry of the compound **3c** in the solid phase is maintained: nine intense peaks are visible for 20 carbons (C_9 and one OCH_3 being superimposed). Surprisingly, a polymorphic transformation occurs with time, while a such kinetic/thermodynamic evolution has never been observed for the other compounds. The thermodynamic polymorph spectrum shows a partial absence of symmetry as underlined by the splitting of C_2, C_9, CH_3 and OCH_3 carbons (SM). This asymmetry may be explained by a movement of the isobutyl side chain. It has to be noted that the two polymorphs give the same ^{13}C liquid state NMR spectrum.

$^{\|}$ Low temperature liquid state experiments were run in CD_2Cl_2 instead of chlorofluorocarbons generally used for this purpose but in which the studied macrocycles were not soluble.

Moreover, the *quasi* absence of intermolecular hydrogen bonding ($\Delta\delta_{CO} = +0.2 - +0.6$ ppm) may be explained by the bulkiness of the two isobutyl substituents while the slight C_7 downfield shift ($\Delta\delta = +1.9 - +2.3$ ppm) agrees with a *trans* conformation, previously assigned by calculations.

The solid state spectrum of compound **4c**, compared with the liquid phase, shows an unsymmetrical conformation in regard to the C_2 axis. While the sites are conformationally averaged in solution to give one resonance, in the solid phase spectrum two resonances of nearly equal intensity are observed for each carbon, except for the C_3 and Ar–CH carbons, the peaks of which are broadened. The asymmetry could be due to different orientations or dynamic motions of the two phenyl rings, which could undergo a staccato-like rotation (or π-flip)[36] and their non-equivalence could result from a lattice deformation corresponding to a minimum space occupation and a minimum repulsion. This observed asymmetry is consistent with the molecular modeling results that indicate for **4c**: (i) different N_4–C_5–C_6–C_7 dihedral angles values between the two chains (Table 5), (ii) the presence of a single NH⋯$O_{1'}$ intramolecular hydrogen bond up to conformer 5 (SM).

Finally, the spectra of the two achiral 3-unsubstitued macrocycles (**6b** and **6c**) were recorded to investigate the influence of the methoxy groups on the 14-membered ring. For these two compounds, the symmetry is conserved in the solid state. The comparison for both compounds of liquid and solid state chemical shifts indicates that in the solid state: (i) intermolecular CO⋯HN hydrogen bonding occurs only in isomer **6c** (**6c**: $\Delta\delta_{CO}$ +1.8 ppm; **6b**: $\Delta\delta_{CO}$ 0 ppm), (ii) a *trans* conformation is conserved along the two bonds $C_{7'}$–O_1–C_2–C_3, while a small γ-*gauche* effect is observed along the two bonds $C_{6'}$–$C_{7'}$–O_1–C_2 referring to the C_2 and C_6 chemical shift variations (Table 6).

Thus it appears from these results that the γ-*gauche* effect observed for **1c** in the solid state is not dictated by the methoxy groups but is induced by the presence of the 3-phenyl substituent.

In summary, ^{13}C SS CPMAS NMR is a simple and useful tool for obtaining conformational data in the solid state. For compound **1c**, the NMR results are consistent with those obtained by the X-ray analysis. More specifically, the NMR technique enabled us to show the presence of: (i) a symmetry in compounds **1c–3c**, **6b** and **6c**, and an asymmetry in compound **4c** in the solid state, (ii) intermolecular CO⋯HN hydrogen bonds for compounds **1a**, **1c–4c** and **6c**, the strength of which decreases with the bulkiness of the substituents, (iii) strong *gauche* conformations for the two $C_{7'}$–O_1–C_2–C_3 bonds in **1c**, and weaker *gauche* conformations for the two $C_{6'}$–$C_{7'}$–O_1–C_2 bonds in **6b** and **6c**, (iv) polymorphic forms for compound **3c**, probably due to the high degree of freedom of the isobutyl side chain.

3. Conclusion

In the liquid state, the conformations of the 14-membered diketal dilactam macrocycles, which all show gg' or g'g arrangements for C_6, $C_{6'}$, seem to depend strongly on whether the molecules are chiral or achiral, and whether the OMe groups are in a *cis* or *trans* configuration. In achiral compounds, the more stable conformation has the two NH–CO links perpendicular to the macrocyclic plane, with orientation either same (in **6c**, **7c**) or opposite (in **6b**, **7b**); this latter arrangement lends to **6b** and **7b** a rectangular [3434]-type structure with the four corners at C_3, $C_{3'}$, C_7, $C_{7'}$. In contrast, in the chiral compounds **1–5**, the conformations are governed: (i) by the presence of one (in most isomers **b**) or two (in most isomers **a** and **c**) N_4–H⋯$O_{1'}$, $N_{4'}$–H⋯O_1 intramolecular hydrogen bonds, which sets the amide function parallel to the macrocyclic plane, (ii) by the position of the OMe groups in regard to the 3-R substituents, (iii) by the nature of the 3-R substituent. Thus the structure tg'ttg'gttg'ttg'gt (Ic), which has no corner, is most frequently observed for 3,3'-monosubstituted compounds **1c–4c**, while no predominant structure appears for the corresponding isomers **a** and **b**.

In the solid state, only slight changes in conformation seem to occur for the achiral compounds **6b** and **6c** in regard to the liquid state; they probably retain the more stable shape found in molecular modeling studies that is the NH–CO link perpendicular to the macrocyclic plane, with, however, in the present case, NH⋯O=C intermolecular hydrogen bonds between successive sheets, H bonds underlined by a small γ effect on the C_2 and C_6 carbons and, in **6c**, slight deshielding of the CO carbon. This orientation of the amide moieties is probably present in the solid state of chiral compounds **1a**, **1b**, **2c–4c** with, however, the cohesive force of any intermolecular H bonds strongly weakened (**1a**, **1b**, **2c**) or cancelled (**3c**, **4c**) by the presence of 3-R substituents. In contrast, in compound **1c**, the cohesion of the NH⋯O=C intermolecular H bonds, revealed by the X-ray analysis, is reinforced by a π–π stacking effect between the phenyl groups, which adopt a position parallel to the macrocyclic plane and thus give to the molecule a constrained shape with an unusual *gauche* conformation along the two $C_{7'}$–O_1–C_2–C_3 bonds.

4. Experimental

4.1. Synthesis

The 14-membered ring diketal dilactam syntheses were previously reported.[1]

4.2. Liquid NMR

Proton and carbon NMR spectra were recorded in deuterio-chloroform solutions using a Bruker AC 400 spectrometer ([1]H: 400 MHz; [13]C: 100 MHz), equipped with a DUAL ^{1}H/^{13}C probe, at 303 K. Chemical shifts are given in parts per million (ppm) and referenced to chloroform ($\delta =$ 7.27 ppm for ^{1}H and 77.1 ppm for ^{13}C) as internal standard.

The NOE measurements were made on a Bruker spectrometer, model DSX 300, equipped with a double resonance probe, at 303 K with 10 mM CDCl$_3$ solutions. Samples were degassed by bubbling dry argon through the solution in the

NMR tube for 30 min. NOE difference spectra were recorded after presaturation of the signal to irradiate using the 'NOEmult' pulse sequence. The following conditions were used: proton relaxation delay 1 s, irradiation period 2.5 s (50 presaturation cycles of 50 ms), total measuring time 7 s. Each FID corresponds to the average of 64 acquisitions and the NOE difference spectra to the average of 8 FID.

4.3. Molecular modeling

The MACROMODEL molecular modeling program (version 7.0) developed by Still and co-workers[38] was used to determined the global minimum conformations of the macrocyclic diketals dilactams. The AMBER force field[39] implemented in the program and well-suited to the study of compounds incorporating amide functions was chosen. The method known as Monte-Carlo Multiple Minimum Search (MCMM) was applied. The starting structure was the previously determined XR structure of the macrocycle 1c.[1a] All other structures were written from the 1c minimum conformation. A minimum of 5000 conformations were minimized for every compound. Detection conditions for hydrogen bonds: interatomic distances $d < 2.5$ Å, angles: N–H⋯O $< 90°$ and H⋯O–R $< 60°$.

4.4. Solid state NMR

The high-resolution ^{13}C solid state spectra were recorded at 75.46 MHz on a Bruker Avance DSX-300 spectrometer with a double bearing magic angle spinning (MAS) probehead. The samples were packed in 4 mm zirconia rotors fitted with Kel-F caps, and when the amount of macrocycle was not sufficient, the sample volume was reduced in the center of the rotor using a Teflon insert. The samples were spun at the magic angle with a speed of 10 kHz at ambient temperature. A ramped cross polarization (RACP) from protons to carbon was carried out at a proton nutation frequency of 70 kHz over a contact time of 1.5 ms and a recycle delay of 3 s. The proton CW decoupling field strength was 68 kHz, and when necessary a TPPM decoupling[40] with a ^{1}H nutation frequency of 70 kHz, a pulse length of 6.0 μs and a phase shift of 15° was used to resolve the asymmetric doublet due to the large ^{14}N quadrupolar coupling. Dipolar dephased spectra were obtained by turning off the ^{1}H decoupling for a short time after the cross-polarization pulse. Also, to suppress the movable methyl groups, the delay was set between 25 and 150 μs depending on the structure. Free induction decays (FID) were digitized into 6 K data points and Fourier-transformed after applying 5 Hz exponential line broadening. The number of transients (200–4096) was fitted to reach optimal signal-to-noise ratios. ^{13}C chemical shifts were measured relative to an external reference (carbonyl of glycine: 176.03 ppm, Aldrich), set carefully before each spectrum.

Supplementary data

Supplementary data associated with this article can be found, in the online version, at doi:10.1016/j.tet.2005.03.073

Tables of: (1) Relative energy (kJ mol^{-1}) of the 10 first conformers of compounds 1–7; (2) H$_3$–C$_3$–C$_2$–H$_2$ and H$_7$–C$_7$–C$_6$–H$_6$ dihedral angles; (3) Interatomic distances between the H$_6$ hydrogens and the OMe oxygens; (4) Interatomic distances between the NH hydrogens and the endocyclic acetalic oxygens.

Solid state ^{13}C NMR chemical shifts of macrocycles 1a–c, 2c–4c, 6b–c and spectra of 1a–c.

References and notes

1. (a) Dugat, D.; Chiaroni, A.; Riche, C.; Royer, J.; Husson, H.-P. *Tetrahedron Lett.* **1997**, *38*, 5801–5804. (b) Valade, A.-G.; Dugat, D.; Jeminet, G.; Royer, J.; Husson, H.-P. *Eur. J. Org. Chem.* **2001**, *11*, 2041–2053.
2. Pointud, Y.; Valade, A.-G.; Pointon, C.; Dugat, D.; Jeminet, G.; Beltran, J.-L. *Supramol. Chem.* **2003**, *15*, 261–269.
3. (a) Dale, J. *J. Chem. Soc.* **1963**, 93–111. (b) Dale, J. *Angew. Chem., Int. Ed. Engl.* **1966**, *5*, 1000–1021.
4. (a) Dale, J. *Acta Chem. Scand.* **1973**, *27*, 1115–1129. (b) Dale, J. *Acta Chem. Scand.* **1973**, *27*, 1130–1148.
5. (a) Anet, F. A. L.; Cheng, A. K.; Wagner, J. J. *J. Am. Chem. Soc.* **1972**, *94*, 9250–9252. (b) Anet, F. A. L.; Cheng, A. K. *J. Am. Chem. Soc.* **1975**, *74*, 2420–2424.
6. Groth, P. *Acta Chem. Scand.* **1976**, *A30*, 155–156.
7. Drotloff, H.; Rotter, H.; Emeis, D.; Möller, M. *J. Am. Chem. Soc.* **1987**, *109*, 7797–7803.
8. Saunders, M. *J. Am. Chem. Soc.* **1987**, *109*, 3150–3152.
9. Shannon, V. L.; Strauss, H. L.; Snyder, R. G.; Elliger, C. A.; Mattice, W. L. *J. Am. Chem. Soc.* **1989**, *111*, 1948–1958.
10. Dunitz, J. D. *Perspectives in Structural Chemistry*; Wiley: New-York, 1968; (a) p 18; (b) p 20.
11. Borgen, G.; Dale, J. *Chem. Commun.* **1970**, 1340–1342.
12. Dale, J. *Acta Chem. Scand.* **1973**, *27*, 1149–1158.
13. Clyne, D. S.; Weiler, L. *Tetrahedron* **2000**, *56*, 1281–1297.
14. Bassi, I. W.; Scordamaglia, R.; Fiore, L. *J. Chem. Soc., Perkin Trans 2* **1972**, 1726–1729.
15. Dunitz, J. D.; Meyer, E. F., Jr. *Helv. Chim. Acta* **1965**, *48*, 1441–1449.
16. Brown, C. J. *J. Chem. Soc. (C)* **1966**, 1108–1112.
17. Anet, F. A. L.; Cheng, A. K.; Krane, J. *J. Am. Chem. Soc.* **1973**, *95*, 7877–7878.
18. Groth, P. *Acta Chem. Scand.* **1975**, *A 29*, 374–380.
19. Borgen, G.; Dale, J. *Acta Chem. Scand.* **1972**, *26*, 1799–1804.
20. Groth, P. *Acta Chem. Scand.* **1979**, *A 33*, 503–513.
21. Wiberg, K. B.; Waldron, R. F.; Schulte, G.; Saunders, M. *J. Am. Chem. Soc.* **1991**, *113*, 971–977.
22. Borgen, G.; Dale, J.; Rise, F.; Gundersen, L.-L. *Magn. Reson. Chem.* **1996**, *34*, 289–292.
23. Dale, J. *Top. Stereochem.* **1976**, *9*, 199–269.
24. Borgen, G.; Dale, J.; Gundersen, L.-L.; Krivokapic, A.; Rise, F.; Overas, A. T. *Acta Chem. Scand.* **1998**, *52*, 1110–1115.
25. Naruse, N.; Konishi, M.; Oki, T.; Inouye, Y.; Kakisawa, H. *J. Antibiot.* **1991**, *44*, 756–761.
26. Hedge, V. R.; Patel, M. G.; Gullo, V. P.; Ganguly, A. K.; Sarre,

O.; Puar, M. S.; McPhall, A. T. *J. Am. Chem. Soc.* **1990**, *112*, 6403–6405.

27. Northolt, M. G.; Alexander, L. E. *Acta Crystallogr.* **1971**, *B27*, 523–531.

28. Dale, J.; Coulon, R. *J. Chem. Soc.* **1964**, 182–187.

29. Laws, D. D.; Bitter, H.-M.L.; Jerschow, A. *Angew Chem., Int. Ed.* **2002**, *41*, 3096–3129.

30. Uhrin, D.; Liptaj, T. *J. Magn. Reson.* **1989**, *8*, 82–91.

31. Morzycki, J. W.; Wawer, I.; Gryszkiewicz, A.; Maj, J.; Siergiejczyk, L.; Zaworska, A. *Steroids* **2002**, *67*, 621–626.

32. Buchanan, G. W.; Kirby, R. A.; Charland, J. P. *J. Am. Chem. Soc.* **1988**, *110*, 2477–2483.

33. Munowitz, M. G.; Griffin, R. G.; Bodenhausen, G.; Huang, T. H. *J. Am. Chem. Soc.* **1981**, *103*, 2529–2533.

34. Hughes, C. E.; Pratima, R.; Karlsson, T.; Levitt, M. H. *J. Magn. Reson.* **2002**, *159*, 25–35.

35. Buchanan, G. W.; Rastegar, M. F. *Solid State Nucl. Magn. Reson.* **2001**, *20*, 137–144.

36. Glaser, R.; Novoselsky, A.; Shiftan, D.; Drouin, M. *J. Org. Chem.* **2000**, *65*, 6345–6353.

37. Scheler, U. In *Solid State NMR Spectroscopy: Principles and Applications*; Duer, M. J., Ed.; Blackwell Science: Oxford, 2002; pp 485–509.

38. Mohamadi, F.; Richards, N. G. J.; Guida, W. C.; Liskamp, R.; Lipton, M.; Caufield, C.; Chang, G.; Hendrickson, T.; Still, W. C. *J. Comput. Chem.* **1990**, *11*, 440–467.

39. Weiner, S. J.; Kollman, P. A.; Nguyen, D. T.; Case, D. A. *J. Comput. Chem.* **1986**, *7*, 230–252.

40. Bennett, A. E.; Rienstra, C. M.; Auger, M.; Lakshmi, K. V.; Griffin, R. G. *J. Chem. Phys.* **1995**, *103*, 6951–6957.